Langmuir

Article

pubs.acs.org/Langmuir

Formation of Cholesterol-Rich Supported Membranes Using Solvent-Assisted Lipid Self-Assembly

Seyed R. Tabaei,[†,‡] Joshua A. Jackman,[†,‡] Seong-Oh Kim,[†,‡] Bo Liedberg,[†,‡] Wolfgang Knoll,[†,‡,⊥] Atul N. Parikh,[†,‡,∥] and Nam-Joon Cho*[,†,‡,§]

[†]School of Materials Science and Engineering, Nanyang Technological University, 50 Nanyang Avenue, Singapore 639798, Singapore

[‡]Centre for Biomimetic Sensor Science, Nanyang Technological University, 50 Nanyang Drive, Singapore 637553, Singapore

[§]School of Chemical and Biomedical Engineering, Nanyang Technological University, 62 Nanyang Drive, Singapore 637459, Singapore

[∥]Department of Biomedical Engineering and of Chemical Engineering & Materials Science, University of California, Davis, California 95616, United States

[⊥]Austrian Institute of Technology (AIT), Donau-City-Strasse 1, 1220 Vienna, Austria

Supporting Information

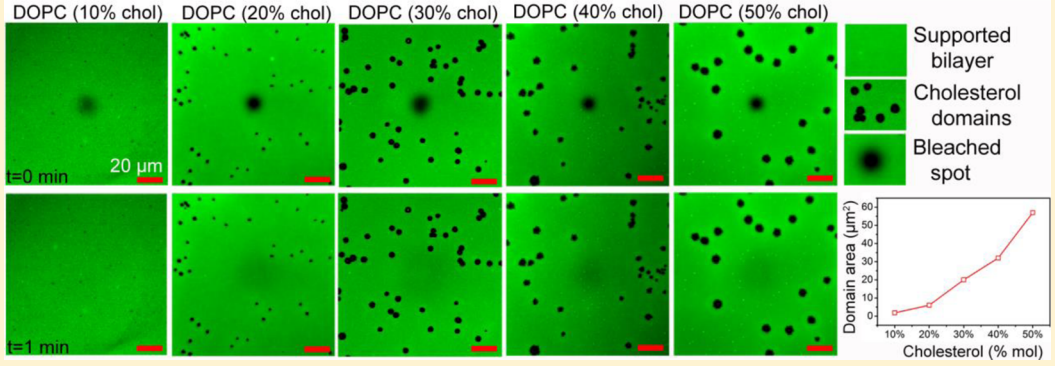

ABSTRACT: This paper describes the application of a solvent-exchange method to prepare supported membranes containing high fractions of cholesterol (up to ∼57 mol %) in an apparent equilibrium. The method exploits the phenomenon of reverse-phase evaporation, in which the deposition of lipids in alcohol (e.g., isopropanol) is followed by the slow removal of the organic solvent from the water-alcohol mixture. This in turn induces a series of lyotropic phase transitions successively producing inverse-micelles, monomers, micelles, and vesicles in equilibrium with supported bilayers at the contacting solid surface. By using the standard cholesterol depletion by methyl-β-cyclodextrin treatment, a quartz crystal microbalance with dissipation monitoring assay confirms that the cholesterol concentration in the supported membranes is comparable to that in the surrounding bulk phase. A quantitative characterization of the biophysical properties of the resultant bilayer, including lateral diffusion constants and phase separation, using epifluorescence microscopy and atomic force microscopy establishes the formation of laterally contiguous supported lipid bilayers, which break into a characteristic domain-pattern of coexisting phases in a cholesterol concentration-dependent manner. With increasing cholesterol fraction in the supported bilayer, the size of the domains increases, ultimately yielding two-dimensional cholesterol bilayer domains near the solubility limit. A unique feature of the approach is that it enables preparation of supported membranes containing limiting concentrations of cholesterol near the solubility limit under equilibrium conditions, which cannot be obtained using conventional techniques (i.e., vesicle fusion).

INTRODUCTION

Cholesterol, a principal component of mammalian cell membranes, is inhomogeneously distributed among various membranes of the cell.[1] The highest cholesterol-containing membranes are generally the plasma membranes,[2] in which the cholesterol concentration can approach 45−50 mol % relative to other lipids (e.g., in erythrocytes). By contrast, intracellular membranes (e.g., in the endoplasmic reticulum, the Golgi apparatus, in lysosomes, and mitochondrial membranes) contain significantly less or no cholesterol. Moreover, in a variety of diseased states, cellular membranes accumulate high concentrations of cholesterol, thereby affecting normal cellular function.[3] The formation of crystalline cholesterol domains in biological membranes at cholesterol concentrations above solubility limits can contribute to abnormal pathologies such as atherosclerosis.[4]

Received: August 27, 2014
Revised: October 2, 2014
Published: October 6, 2014

   dx.doi.org/10.1021/la5034433 | Langmuir 2014, 30, 13345−13352

A major way by which cholesterol modulates the functions of a cellular membrane is by affecting its physical properties. A wealth of previous efforts employing model membranes establish that the presence of cholesterol influences spatial distribution of membrane components by promoting domain formation within single membranes because of its differential affinity for saturated lipids and sphingomyelin.[5,6] Moreover, cholesterol has a strong ordering effect on membrane phospholipids by influencing the gel to liquid-crystalline phase transition and altering membrane fluidity (or rigidity).[7] With increasing knowledge about the nonideal mixing of phospholipids and cholesterol, it is becoming increasingly apparent that the structural properties and phase behavior[8−10] are strongly dependent on the type (or state) of the model membrane (e.g., monolayer,[11] bilayer,[7] multilayer film,[12] and giant vesicle[13]).

Because of their versatility for practical applications (i.e., biosensor development) and amenability for characterization by using surface-sensitive measurement techniques,[14,15] developing a means to prepare complex supported membranes and understanding their structural and phase behavior is important. At the same time, studies of supported membranes containing high concentrations of cholesterol are sparse presumably because of the challenges associated with preparing such membranes. The primary method available to form cholesterol-rich supported bilayers is Langmuir-type transfer processes that involve two successive transfers of lipid monolayers.[7] However, it is difficult to produce equilibrium bilayer phases by this approach[16,17] because of the lack of alignment between domains found in the two leaflets.[16] Alternatively, vesicle fusion, another widely used method to prepare supported bilayers, can be employed.

The vesicle fusion approach involves adsorption, spontaneous rupture, and spreading of precursor small unilamellar vesicles (∼100 nm diameter) on a solid support.[18] However, the preparation of small vesicles containing high cholesterol concentrations leads to substantial heterogeneity in the compositions of individual vesicles[19,20] and different fusion rates of different subpopulations of vesicles, all of which complicate the fusion process often resulting in supported membranes whose compositions vary significantly from the parent lipid stock.[21] Moreover, supported bilayers containing high cholesterol fractions are difficult to prepare[22] because cholesterol-rich vesicles have higher apparent transition temperatures and appreciably larger bending rigidities that hinder vesicle formation and rupture[23] (in some cases,[24,25] formation of discontinuous bilayer patches is reported). As such, using the vesicle fusion method, only bilayers containing 20−30 mol % cholesterol can be reproducibly prepared. For vesicles containing higher cholesterol fractions, alternate approaches that facilitate vesicle rupture, such as by addition of a membrane-active peptide[26,27] or application of hydrodynamic force,[28,29] have proved successful, although these methods are rather complicated, require additional technical resources, and the corresponding mechanisms remain poorly understood.

In an independent membrane preparation method that does not require vesicles, Hohner et al. reported a gradual solvent-exchange process to form planar supported bilayers[30] of simple lipid composition on silicon oxide, termed here the solvent-assisted lipid bilayer (SALB) method. The method exploits the phenomenon of reverse-phase evaporation in which the deposition of lipids in alcohol (e.g., isopropanol) is followed by the slow removal of the organic solvent (i.e., alcohol) from the water-alcohol mixture which induces a series of lyotropic phase transitions successively producing inverse-micelles, monomers, micelles, and vesicles in equilibrium with supported bilayers at the contacting solid surface.[30,31] A key feature of the SALB method is that the process does not require preformed precursor vesicles, which is particularly valuable as it enables, in principle, the SALB method to be applicable to lipid mixtures and compositions for which vesicle formation (and fusion) is difficult. Similar approaches[32,33] have also been utilized to form tethered lipid bilayers on solid supports. Here, using a modified version of the SALB method that was recently developed by our group,[34] we investigate preparation and characterization of supported bilayers containing variable concentrations of cholesterol.

MATERIALS AND METHODS

Sample Preparation. A zwitterionic lipid, 1,2-dioleoyl-*sn*-glycero-3-phosphocholine (DOPC), cholesterol (Chol), and fluorescently labeled lipid, 1,2-dioleoyl-*sn*-glycero-3-phosphoethanolamine-*N*-(lissamine rhodamine B sulfonyl) (ammonium salt) (Rhodamine-DHPE), were purchased from Avanti Polar Lipids (Alabaster, AL). Immediately prior to the experiment, the lipid powder was dissolved in isopropanol at 10 mg mL^{-1} lipid concentration, mixed to the desired DOPC:Chol molar ratio, and then diluted to a 0.5 mg mL^{-1} lipid concentration. The aqueous buffer solution was 10 mM Tris buffer solution [pH 7.5] with 150 mM NaCl. In fluorescence microscopy experiments, the lipid composition also contained 0.5 wt % Rhodamine-DHPE. Small unilamellar vesicles were prepared as follows: dried lipid films were rehydrated in aqueous buffer solution at a nominal lipid concentration of 5 mg mL^{-1}. The hydrated lipid films were then extruded through 50 nm diameter track-etched polycarbonate membranes in order to form small unilamellar vesicles, as previously described.[35]

Epifluorescence Microscopy. Epifluorescence microscopy imaging was performed using an inverted epifluorescence Eclipse TE 2000 microscope (Nikon) equipped with a 60× oil immersion objective (NA 1.49) and an Andor iXon+ EMCCD camera (Andor Technology, Belfast, Northern Ireland). The acquired images had dimensions of 512 × 512 pixels with a pixel size of 0.267 × 0.267 μm. The samples were illuminated through a TRITC (Rhodamine−DHPE) filter set by a mercury lamp (Intensilight C-HGFIE; Nikon Corporation). For fluorescence recovery after photobleaching (FRAP) analysis, a 30 μm wide circular spot was photobleached with a 532 nm, 100 mW laser beam, followed by time-lapsed recording. The bleaching time was 5 sec. The recovery was followed for 60 sec at 1 sec intervals, and diffusion coefficients were computed using the Hankel transform method.[36] All image processing was done using ImageJ. For bilayer formation using the SALB procedure, commercially available microfluidic flow cells (stick-Slide I0.1 Luer, Ibidi, Munich, Germany) were employed, with an injection flow rate of 50 μL min^{-1}.

Atomic Force Microscopy. An NX-Bio atomic force microscope (Park Systems, Suwon, South Korea), combined with an Eclipse Ti optical microscope (Nikon, Tokyo, Japan), was employed to image SALB experimental samples in the contact mode. An ultrasharp, silicon nitride BioLever mini cantilever tip (Olympus, Tokyo, Japan) was used for all experiments. The tip has a tetrahedral shape, 110 kHz resonance frequency, and a 0.09 N m^{-1} spring constant. Prior to the experiments, the tip was subjected to oxygen plasma treatment at maximum radio frequency power (Harrick Plasma, Ithaca, New York) for 5 min and sequentially rinsed with ethanol (70%), ultrapure water, and ethanol (70%) before finally drying with a gentle stream of nitrogen air. Experiments were conducted in an acoustic enclosure (Park Systems) with a temperature controller set at a constant temperature of 25 °C. AFM imaging was done on SALB samples immediately after QCM-D experiment and postrinsing with 10 mM Tris buffer [pH 7.5] with 150 mM NaCl.

Quartz Crystal Microbalance-Dissipation. A Q-Sense E4 instrument (Q-Sense AB, Gothenburg, Sweden) was employed to

dx.doi.org/10.1021/la5034433 | *Langmuir* 2014, 30, 13345−13352

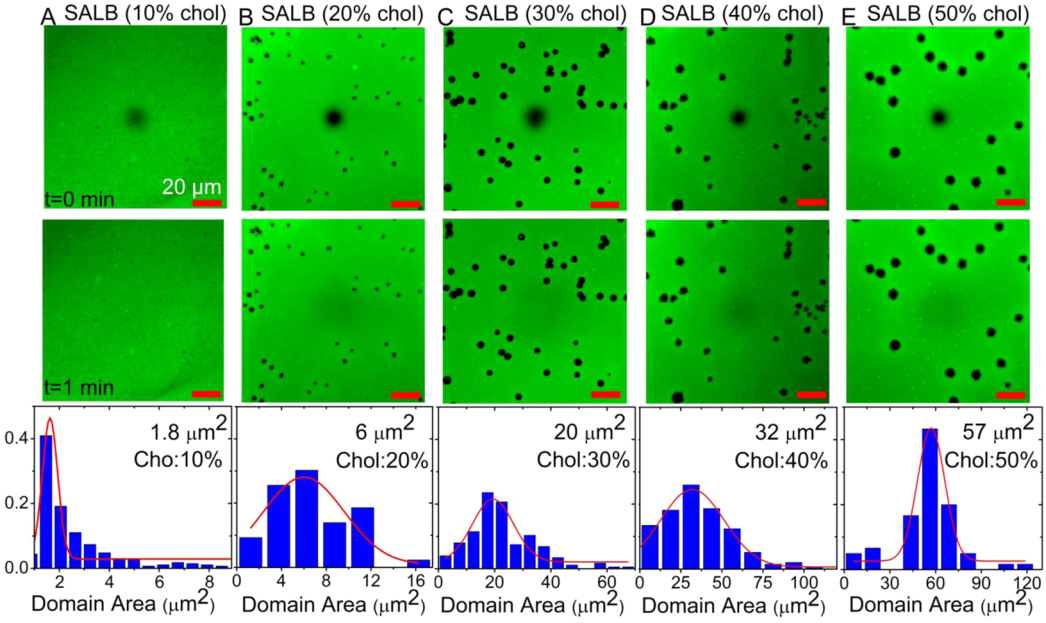

Figure 1. Observation of fluidic cholesterol-enriched supported membranes on glass. (A–E) Fluorescence micrographs were recorded for supported lipid bilayers formed on a glass substrate. The precursor mixture in isopropanol solution had a molar ratio of $(100 - x)$ mol % DOPC lipid and x mol % Chol and contained 0.5 wt % fluorescent Rhodamine-PE lipid; x ranged from 0 to 50 mol %. Images were recorded immediately (top) and 1 min (middle) after photobleaching. The dark spot in the image center corresponds to the photobleached region. The scale bars are 20 μm. Surface area histograms of individual dye-excluded domains within each sample are also presented (bottom).

monitor the adsorption kinetics of lipids onto silicon oxide- and gold-coated 5 MHz, AT-cut piezoelectric quartz crystals. Changes in frequency (Δf) and energy dissipation (ΔD) were recorded as functions of time, as previously described.[37] The measurement data was collected at the $n = 3-11$ odd overtones, with the reported values having been recorded at the third overtone. The normalized values ($\Delta f_{n=3}/3$) are reported in this study. All samples were introduced at a flow rate of 50 μL min^{-1} using a peristaltic pump (Ismatec Reglo Digital) under continuous flow conditions. The temperature of the flow cell was fixed at 24.00 ± 0.5 °C. Before the experiments, the sensor surfaces were treated with oxygen plasma at maximum radio frequency power (Harrick Plasma) for 1 min immediately before use.

RESULTS

Using the SALB method, we prepared DOPC/Chol lipid bilayers containing variable fractions of cholesterol (between 0 and 50 mol % Chol in the precursor mixture) on a silicon oxide substrate. The precursor mixture of phospholipid and Chol in isopropanol solution was incubated in the measurement chamber for a minimum of 10 min, and then aqueous buffer solution was flowed-through the chamber to facilitate solvent-exchange. A small fraction (0.5 wt %) of fluorescent Rhodamine-DHPE lipid was included in the mixture in order to visualize the bilayer phase formed on the substrate by epifluorescence microscopy. Preliminary quartz crystal microbalance with dissipation monitoring (QCM-D) measurements reveal that the final frequency and energy dissipation shifts are −25.3 ± 3.4 Hz and 0.7 ± 0.7 × 10^{-6}, respectively (Figure S1 of the Supporting Information), which, based on previous reports,[22,27] confirms that the SALB process produces single supported bilayers at the substrate surface comparable in surface density to those formed by vesicle fusion and by the Langmuir-Blodgett method.

Typical epifluorescence micrographs (100 × 100 μm) are presented in Figure 1 for the supported membranes formed on silicon oxide following completion of the SALB procedure. The micrographs reveal the formation of a membrane phase, characterized by a uniform fluorescence intensity consistent with the formation of a single lipid bilayer. In addition to the phospholipid-rich phase, there are dye-excluded circular spots distributed randomly throughout the membrane phase (Figure 1), which are largely monodisperse in single samples and stable over long periods of time. Because Rhodamine-DHPE partitions preferentially in the fluid phase, we tentatively ascribe the dye-decorated surroundings to the cholesterol-depleted, phospholipid rich fluid phase and the dark spots to the cholesterol-enriched dense phase. In order to determine if the phase-separating supported membrane morphologies exhibit long-range lateral diffusion (and fluid character), we carried out a microscope-based FRAP experiment. In Figure 1, upper and lower micrographs are captured at t = 0 and 1 min after bleaching, respectively. For all cholesterol concentrations, near-complete recovery of the photobleached spot suggests that the dye-laden, cholesterol-depleted phase is indeed laterally fluid.

This assignment is further consistent with the fact that the sizes of the dye-depleted domains increase with the cholesterol content. With increasing Chol fraction in the precursor mixture, the average domain size increases from 1.8 μm^2 for 10 mol % Chol to 57 μm^2 for 50 mol % Chol. As expected, no dye-excluded domains are apparent in a single component DOPC lipid bilayer also formed by the SALB procedure (Figure S2 of the Supporting Information). We also prepared DOPC/Chol membranes on the same substrates through conventional vesicle fusion. Although the preparation of uniform bilayer samples with high cholesterol concentrations (>20%) was erratic and irreproducible (Figure S3 of the Supporting Information), supported membrane samples obtained using vesicles containing 20 mol % Chol or less also revealed dark circular domains similar to those observed in samples prepared

dx.doi.org/10.1021/la5034433 | Langmuir 2014, 30, 13345–13352

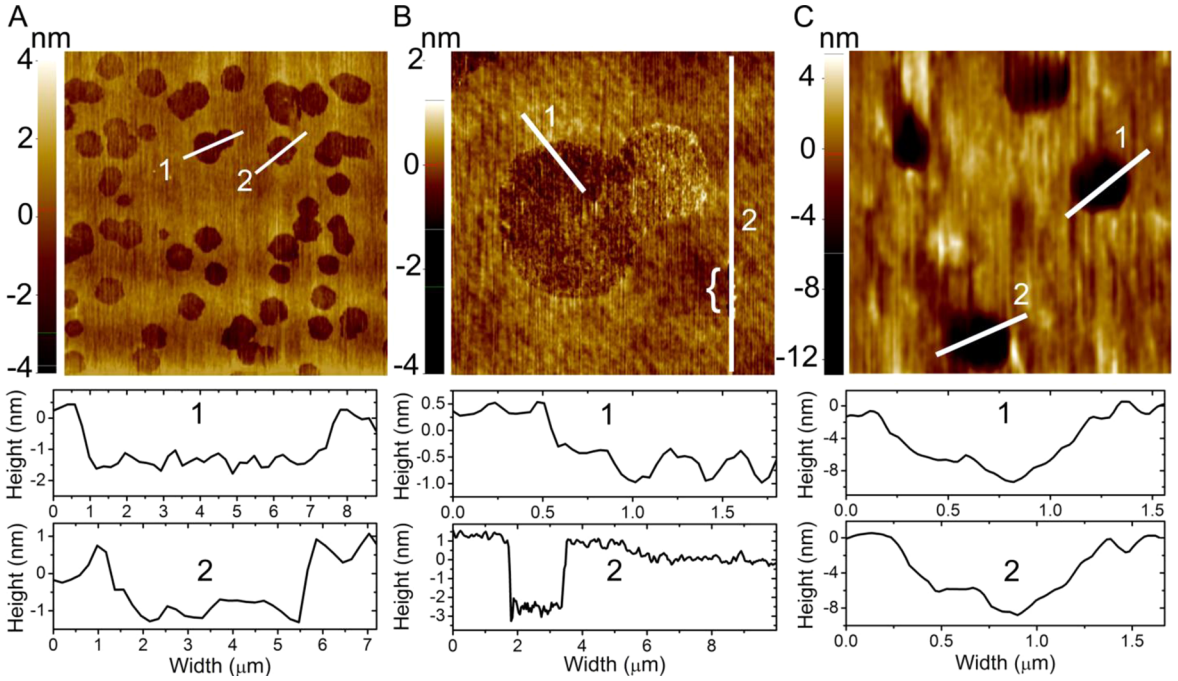

Figure 2. Characterization of dye-excluded domains by tapping mode atomic force microscopy. (A) AFM height mode image of a SALB-formed supported lipid bilayer. The composition of the precursor mixture was 70 mol % DOPC lipid and 30 mol % cholesterol. The scan size was 50 × 50 μm. Two line scans are denoted by labels 1 and 2, respectively, and the corresponding height profiles are presented below the AFM images. (B) AFM height mode image of a representative dye-excluded domain. The scan size was 10 × 10 μm. Two line scans are denoted by labels 1 and 2, respectively. The "1" line scan was performed to determine the height difference between the phospholipid-rich phase and dye-excluded domain. The "2" line scan was performed to determine the thickness of the phospholipid-rich phase. (C) AFM height mode image of a lipid bilayer defect created by treatment with 1 mM MβCD. The image was recorded postrinse 30 min after MβCD application, and the scan size was 5 × 5 μm. Two line scans are denoted by labels 1 and 2, respectively, and the corresponding height profiles are presented.

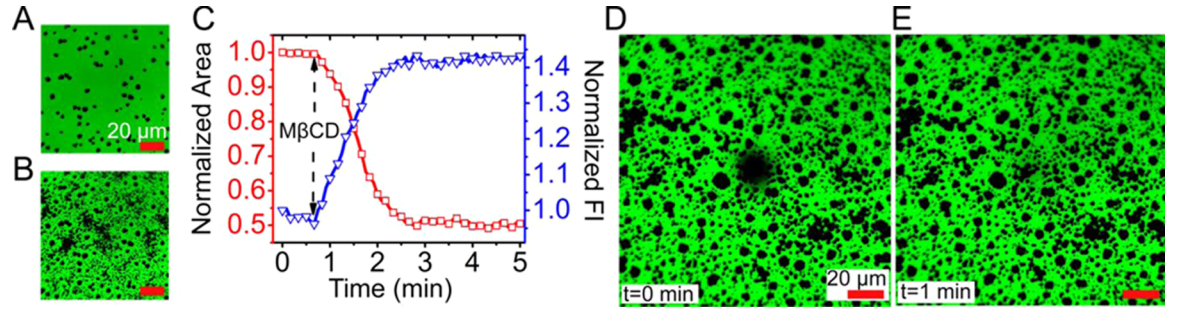

Figure 3. Cholesterol depletion by methyl-β-cyclodextrin treatment. Fluorescence micrograph of a cholesterol-enriched supported membrane (A) before and (B) after treatment with 1 mM MβCD. The precursor mixture was 50 mol % DOPC and 50 mol % Chol and contained 0.5 wt % Rhodamine-PE. (C) Time-lapsed fluorescence microscopy imaging was performed in order to measure the effects of 1 mM MβCD treatment on the lipid bilayer region in panels A and B. The total surface area of the bilayer region (green color) and average fluorescence intensity (FI) of pixels in those regions are presented as a function of time upon MβCD injection (see arrow). (D and E) FRAP analysis on a representative MβCD-treated bilayer is presented. The precursor mixture was 49.5 mol % DOPC, 0.5 wt % Rhodamine-PE, and 50 mol % cholesterol. In panel D, photobleaching was performed at t = 0 min. In panel E, recovery of the fluorescence intensity in the fluid phase regions is observed by t = 1 min.

by the SALB process (Figure S4 of the Supporting Information, panels A and B).

In order to further characterize the dye-excluded domains, we performed independent atomic force microscopy (AFM) experiments. Figure 2 shows representative AFM micrographs for SALB-prepared DOPC/Chol bilayers contraining 30 mol % Chol fraction. Consistent with large-area fluorescence images, the dye-excluded domains are nearly circular in shape, occasionally present as two or more coalescing domains. Line scans across the domain edges show that the phospholipid-rich phase is ~1.5 nm thicker than the dye-excluded domains. The thickness of the phospholipid-rich phase was determined to be ~4.5 nm, so the dye-excluded domains are ~3 nm thick consistent with the presence of a cholesterol-enriched membrane domain. Additional support for the presence of the cholesterol-rich phase in circular domains is obtained through a cholesterol extraction assay. Using 1 mM methyl-β-cyclodextrin (MβCD), which is a cyclic oligosaccharide that removes Chol from lipid bilayers,[38] we found that the height difference between the surrounding membrane phase and the dye-excluded domains substantially increases to between 5 and 8 nm (Figure 2C). This finding indicates that MβCD treatment removes Chol from the dye-excluded domains and also appears to perturb the edge of the membrane phase surrounding the

dx.doi.org/10.1021/la5034433 | *Langmuir* 2014, 30, 13345−13352

Table 1. Fluorescence Recovery Photobleaching (FRAP) Analysis of Lateral Lipid Diffusion in Cholesterol-Enriched Supported Membranes[a]

method	treatment	0% chol	10% chol	20% chol	40% chol	50% chol
SALB	− MβCD	2.32 ± 0.20	2.10 ± 0.15	1.10 ± 0.15	1.12 ± 0.15	0.73 ± 0.19
	+ MβCD	2.32 ± 0.14	2.40 ± 0.15	2.56 ± 0.15	2.45 ± 0.41	2.13 ± 0.29
vesicle fusion	− MβCD	2.42 ± 0.15	2.29 ± 0.16	1.86 ± 0.15	nil	nil
	+ MβCD	2.50 ± 0.20	2.74 ± 0.15	2.67 ± 0.14	nil	nil

[a]The diffusion coefficient (in units $\mu m^2\ s^{-1}$) of lateral lipid mobility is reported for supported membranes with varying DOPC:Chol molar ratios (n = 10 measurements). FRAP measurements were performed before and after 1 mM MβCD treatment. Supported lipid bilayers on glass were formed by either the SALB or vesicle fusion method.

Chol-rich domains. Taken together, the AFM data lend strong, direct support to our foregoing inference that the dye-excluded domains are highly enriched in cholesterol and not voids.

Interestingly, fluorescence micrographs of a 50 mol % Chol-containing lipid bilayer before and after 1 mM MβCD treatment further demonstrate significant alterations in membrane properties in the phospholipid-rich phase as well (Figure 3, panels A and B). Time-resolved measurements of the fluorescent properties of the lipid bilayer show that the surface area of the phospholipid-rich phase decreases by ∼50% upon treatment, and there is a corresponding increase in the normalized fluorescence intensity per unit of surface area by ∼46% (Figure 3C). On the basis of this observation, we infer that at elevated cholesterol content (50 mol %), MβCD treatment removes cholesterol from both the dye-excluded domains and the phospholipid-rich phase. This is consistent with previous studies,[11] which suggest that at high cholesterol contents in the so-called β phase, cholesterol associates with the lipids in a manner that produces a unique phase coexistence between cholesterol−lipid complexes in one phase and free cholesterol associated with the phospholipid-rich phase in the other. Note also that the original shapes of the dye-excluded domains is retained after cholesterol removal, presumably because of reduced bilayer density due to cholesterol extraction, and limits on lateral expansion[39] preclude the necessary spreading of the remainder of the supported bilayer. In order to measure the lateral fluidity of the phospholipid-rich phase before and after cholesterol removal, we further carried out fluorescence recovery after photobleaching (FRAP) experiments and the results were analyzed by the Hankel transform method. Representative fluorescence micrographs, presented for 50 mol % Chol-containing lipid bilayer after MβCD treatment (Figure 3, panels D and E), confirm the retention of long-range fluidity and lateral fluidity of the residual, cholesterol-depleted membrane.

We now report the FRAP experimental results for all membrane compositions before MβCD treatment (Table 1). At low Chol fractions (0−10 mol %) in the precursor mixture, the lateral diffusion coefficient for lipid bilayers was around 2.2 $\mu m^2\ s^{-1}$. With increasing Chol fraction (20−40 mol %), the diffusion coefficients are approximately 1.1 $\mu m^2\ s^{-1}$. Finally, at high Chol fraction (50 mol %), the diffusion coefficient is lowered to 0.8 $\mu m^2\ s^{-1}$. Following MβCD treatment, the diffusion coefficient of all lipid bilayers is between 2.2 and 2.6 $\mu m^2\ s^{-1}$ (Table 1). The results support that MβCD treatment removes Chol from the phospholipid-rich phase and enabled us to quantitatively determine the mole fraction of Chol in the lipid bilayer as explained below.

QCM-D tracking allows us to measure the negative frequency shift ($\Delta f_{bilayer}$) associated with a planar lipid bilayer on silicon oxide. The bilayers have low-energy dissipation ($\Delta D_{Bilayer} < 1 \times 10^{-6}$) so we converted the frequency shift into adsorbed mass ($\Delta m_{Bilayer}$) based on the Sauerbrey relationship.[40] We assume that the bilayer mass represents the sum of DOPC lipid (Δm_{Lipid}) and Chol (Δm_{Chol}) masses. After bilayer formation, 1 mM MβCD was then added in order to observe the positive frequency shift ($\Delta f_{chol} \propto \Delta m_{Chol}$) associated with Chol removal. The results of the MβCD treatment step are presented in Figure 4A. The initial baseline values are the

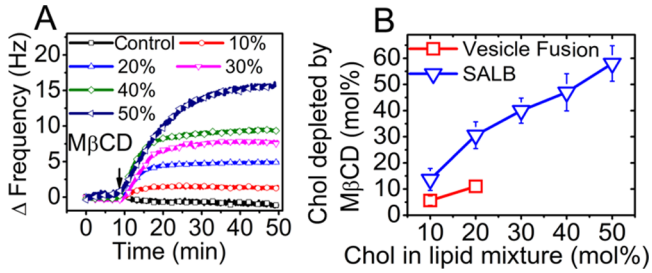

Figure 4. Quantitative determination of cholesterol fraction in supported membranes. (A) The amount of cholesterol incorporated within supported DOPC:Chol lipid bilayers on silicon oxide was determined by QCM-D measurement. First, the SALB procedure was performed to form supported lipid bilayers with varying mole fractions of cholesterol in the precursor mixture (between 0 and 50 mol %). After bilayer formation, the QCM-D frequency shift was then normalized with Δf = 0 Hz corresponding to the supported lipid bilayer in each experiment. One mM MβCD was next added (see arrow) in order to extract cholesterol from the bilayer, and the observed positive frequency shift was due to cholesterol removal from the bilayer. (B) Mole percent of cholesterol depleted from the bilayers prepared by the SALB method as a function of cholesterol fraction in the precursor mixture. For comparison, identical experiments were performed using supported lipid bilayers prepared by the vesicle fusion method.

normalized frequency shifts for the bilayers (defined as $\Delta f_{bilayer}$ = 0). With increasing Chol fraction in the precursor mixture, Δf_{chol} increased proportionally and demonstrated that the cholesterol fraction in the bilayer can be tuned according to the cholesterol fraction in the precursor mixture. The kinetics of Chol removal show first-order features that are consistent with previous reports.[38,41,42] In order to calculate the mole fraction of cholesterol in the bilayer, we determined Δf_{lipid} based on the difference between $\Delta f_{bilayer}$ and Δf_{chol}, applied the Sauerbrey relationship, and took the molecular weights of DOPC lipid and cholesterol into account.

Overall, the calculated mole fractions of Chol in the bilayer demonstrate that the SALB procedure forms Chol-enriched bilayers, which reflect the starting precursor compositions (Figure 4B). There is a nearly linear correspondence between the Chol fraction in the precursor mixture and the Chol fraction in the bilayer, with a slight increase in the Chol fraction

dx.doi.org/10.1021/la5034433 | Langmuir 2014, 30, 13345−13352

in the bilayer. Importantly, the SALB procedure was also successful at forming supported bilayers on gold with similarly high levels of Chol (Figure S5 of the Supporting Information). For comparison, we also formed supported bilayers from vesicles containing up to 20 mol % Chol (i.e., the highest Chol fraction at which vesicles can still rupture spontaneously) and measured the Chol fraction in these bilayers by the same approach. Strikingly, the Chol fraction in these bilayers was appreciably lower than in the precursor vesicles and a maximum fraction of Chol in the bilayers was approximately 10 mol % (see Figure 4B and Figure S5 of the Supporting Information).

In order to form supported bilayers with greater Chol fractions via vesicle rupture, we also employed an amphipathic, α-helical (AH) peptide in order to rupture a layer of adsorbed vesicles that were prepared from parent lipid stocks containing between 30−50 mol % Chol (Figure S6 of the Supporting Information). As described in Introduction, a similar strategy based on peptide-induced vesicle rupture was previously reported by Hardy et al. in order to form planar bilayers with HIV virus-mimicking lipid compositions.[27] While the specific cholesterol fraction in the vesicles in solution was not explicitly determined in our measurements, there was likely at least 20 mol % cholesterol in the DOPC lipid vesicles because the vesicles did not rupture spontaneously upon adsorption onto silicon oxide. After formation of the saturated vesicle adlayer, the AH peptide was added, inducing vesicle rupture and the formation of a supported lipid bilayer in each case. However, surprisingly, we determined that the Chol in the bilayers formed, if present, is intractable to MβCD treatment (no Chol removal), suggesting that either there is no Chol in bilayers formed via this route or more likely that the peptide interferes with membrane properties. Taken together, the data support that the SALB procedure can form supported lipid bilayers containing high fractions of Chol (at least five-fold greater than alternative vesicle fusion methods), and that Chol is present in both the phospholipid-rich phase and cholesterol-rich domains at elevated concentrations.

DISCUSSION

By inducing supported bilayer formation via solvent-exchange, intrinsic challenges imposed by vesicle configurations (e.g., compositional heterogeneity, vesicle stability, and high bending rigidities) are bypassed, allowing the formation of supported bilayers through solvent-assisted lipid self-assembly. To some extent, our strategy also shares a common feature with Langmuir-type transfer processes (i.e., lamellar phase lipid organization at an interface due to water contact), albeit there is one key advantage of the SALB approach for studying phospholipid-cholesterol mixtures. The formation of lamellar phase lipid structures directly proceeds to the bilayer configuration, and the corresponding self-assembly process is also influenced by molecular interactions between the two leaflets. Similar advantages have also been previously described for an analogue of the SALB method termed rapid solvent exchange,[20] which is used to prepare lipid vesicles containing high fractions of cholesterol. As a result, we were able to make several new findings related to phospholipid-cholesterol mixtures in supported bilayers.

In fluid-phase DOPC containing lipid bilayers, cholesterol is located within the fluidic phospholipid-rich phase as well as in micron-scale cholesterol bilayer domains. The effects of cholesterol on the phospholipid-rich phase were consistent with expectations (e.g., decreased fluidity with increased cholesterol fraction). The ability of the SALB approach to prepare supported membranes containing high cholesterol concentrations up to the solubility limit of cholesterol in the lipid phase should prove useful in characterizing the high-concentration β-phase. In principle, the approach should also enable characterization of cholesterol bilayer domains (CBDs) as described by Raguz and colleagues[43,44] (see, for example, refs 45 and 46 for evidence of CBDs in cellular membranes), which appear to be produced beyond the solubility limit when cholesterol crystallizes within the two-dimensional lipid environment. These CBDs are believed to be precursors of crystalline cholesterol yet remain dynamic which might explain the susceptibility of cholesterol-rich, dye-excluded domains to MβCD treatment in this study. Furthermore, we attempted to form crystalline deposits on silicon oxide by performing the SALB procedure from cholesterol alone and without DOPC lipid. In this case, no adsorbed layer was formed after solvent-exchange, which is consistent with the fact that CBDs only form in conjunction with phospholipid-rich phases.[43]

Regarding the molar fraction of cholesterol in the supported bilayers, we were able to directly measure this value by QCM-D measurement. Specifically, we determined the mass of the supported bilayer containing DOPC lipid and cholesterol, removed the cholesterol via MβCD treatment, and then determined again the mass of the remaining adsorbed lipid. To validate this approach, epifluorescence microcopy and AFM measurements verified that MβCD treatment removes cholesterol from both the phospholipid-rich phase and the cholesterol bilayer domains, and the desorption kinetics show first-order features. Radhakrishnan et al. previously showed that the monoexponential decay is related to the chemical activity of cholesterol and the stoichiometric composition of condensed complexes of cholesterol and phospholipid.[41] After MβCD treatment, the residual lipid bilayers had a nearly consistent rate of lateral lipid diffusion, which agrees well with recent work reported by Simonsson and Höök.[29] Furthermore, MβCD treatment had no effect on DOPC lipid bilayers, thus confirming its specific removal of cholesterol.

Importantly, this approach allowed us to determine that the fraction of cholesterol which can be incorporated into the supported bilayer is more than 5 times greater than that permissible with conventional techniques for supported bilayer formation (e.g., vesicle fusion). The molar fraction of cholesterol in supported bilayers formed by the vesicle fusion method was appreciably lower than that of the precursor vesicles, although the molar fraction of the supported bilayer and precursor vesicles are typically assumed to be equivalent.[47,48] Interestingly, we also found that peptide-induced rupture of cholesterol-containing, adsorbed vesicles yielded supported lipid bilayers that were intractable to MβCD treatment. This evidence suggests one of two possibilities. First, the vesicles may not have contained cholesterol due to mixing heterogeneities, however, the complete absence of cholesterol is unlikely and also the vesicles did not rupture spontaneously on silicon oxide. Second, the peptide may not be completely removed from the bilayer or somehow induce cholesterol in the bilayer to assume a highly ordered, functionally inactive state.

CONCLUSION

In this work, we have demonstrated the self-assembly formation and quantitative investigation of fluidic supported lipid bilayers containing high fractions of cholesterol (up to ∼57 mol %).

Considering all of the aforementioned points, the SALB method and its technically minimal requirements is ideally suited to preparing cholesterol-rich supported bilayers. In turn, all of these capabilities should further increase understanding of the ways in which physiologically relevant, elevated levels of cholesterol influence membrane biophysical properties, including membrane fluidity and spatial organization into domain structures (i.e., lipid rafts). Furthermore, the SALB method has strong potential to be explored for coating nanomaterials with physiologically relevant membrane compositions, an opportunity which has so far eluded conventional methods for preparing supported membranes.

■ ASSOCIATED CONTENT

Supporting Information

More detailed information is provided about QCM-D tracking of supported membranes formed via the SALB and vesicle fusion methods (Figures S1 and S3), epifluorescence microscopy images of supported membranes formed via the SALB and vesicle fusion methods (Figures S2 and S4), and QCM-D characterization of cholesterol content in supported lipid bilayers (Figures S5 and S6). This material is available free of charge via the Internet at http://pubs.acs.org.

■ AUTHOR INFORMATION

Corresponding Author

*E-mail: njcho@ntu.edu.sg.

Notes

The authors declare no competing financial interest.

■ ACKNOWLEDGMENTS

This work was supported by the National Research Foundation (NRF-NRFF2011-01) and the National Medical Research Council (NMRC/CBRG/0005/2012). J.A.J. is a recipient of the Nanyang President's Graduate Scholarship.

■ REFERENCES

(1) Van Meer, G.; Voelker, D. R.; Feigenson, G. W. Membrane lipids: Where they are and how they behave. *Nat. Rev. Mol. Cell Biol.* **2008**, *9* (2), 112−124.

(2) Bloch, K. Cholesterol: Evolution of Structure and Function. *Biochem. Lipids, Lipoproteins Membr. (5th Ed.)* **1991**, *20*, 363−381.

(3) Qin, C.; Nagao, T.; Grosheva, I.; Maxfield, F. R.; Pierini, L. M. Elevated Plasma Membrane Cholesterol Content Alters Macrophage Signaling and Function. *Arterioscler., Thromb., Vasc. Biol.* **2006**, *26* (2), 372−378.

(4) Preston Mason, R.; Tulenko, T. N.; Jacob, R. F. Direct Evidence for Cholesterol Crystalline Domains in Biological Membranes: Role in Human Pathobiology. *Biochim. Biophys. Acta, Biomembr.* **2003**, *1610* (2), 198−207.

(5) Brown, D. A.; London, E. Structure and Function of Sphingolipid-and Cholesterol-Rich Membrane Rafts. *J. Biol. Chem.* **2000**, *275* (23), 17221−17224.

(6) Simons, K.; Vaz, W. L. Model Systems, Lipid Rafts, And Cell Membranes 1. *Annu. Rev. Biophys. Biomol. Struct.* **2004**, *33*, 269−295.

(7) Crane, J. M.; Tamm, L. K. Role of Cholesterol in the Formation and Nature of Lipid Rafts in Planar and Spherical Model Membranes. *Biophys. J.* **2004**, *86* (5), 2965−2979.

(8) Ziblat, R.; Kjaer, K.; Leiserowitz, L.; Addadi, L. Structure of cholesterol/lipid ordered domains in monolayers and single hydrated bilayers. *Angew. Chem., Int. Ed.* **2009**, *48* (47), 8958−8961.

(9) Ziblat, R.; Leiserowitz, L.; Addadi, L. Crystalline domain structure and cholesterol crystal nucleation in single hydrated DPPC: cholesterol: POPC bilayers. *J. Am. Chem. Soc.* **2010**, *132* (28), 9920−9927.

(10) Ziblat, R.; Leiserowitz, L.; Addadi, L. Crystalline Lipid Domains: Characterization by X-Ray Diffraction and their Relation to Biology. *Angew. Chem., Int. Ed.* **2011**, *50* (16), 3620−3629.

(11) Ege, C.; Ratajczak, M. K.; Majewski, J.; Kjaer, K.; Lee, K. Y. C. Evidence for lipid/cholesterol ordering in model lipid membranes. *Biophys. J.* **2006**, *91* (1), L01−L03.

(12) Hung, W.-C.; Lee, M.-T.; Chen, F.-Y.; Huang, H. W. The condensing effect of cholesterol in lipid bilayers. *Biophys. J.* **2007**, *92* (11), 3960−3967.

(13) Veatch, S. L.; Keller, S. L. Separation of liquid phases in giant vesicles of ternary mixtures of phospholipids and cholesterol. *Biophys. J.* **2003**, *85* (5), 3074−3083.

(14) Sackmann, E. Supported membranes: scientific and practical applications. *Science* **1996**, *271* (5245), 43−48.

(15) Chan, Y.-H. M.; Boxer, S. G. Model membrane systems and their applications. *Curr. Opin. Chem. Biol.* **2007**, *11* (6), 581−587.

(16) Stottrup, B. L.; Veatch, S. L.; Keller, S. L. Nonequilibrium behavior in supported lipid membranes containing cholesterol. *Biophys. J.* **2004**, *86* (5), 2942−2950.

(17) Watkins, E. B.; Miller, C. E.; Liao, W. P.; Kuhl, T. L. Equilibrium or Quenched: Fundamental Differences between Lipid Monolayers, Supported Bilayers, and Membranes. *ACS Nano* **2014**, *8* (4), 3181−3191.

(18) Richter, R. P.; Bérat, R.; Brisson, A. R. Formation of solid-supported lipid bilayers: an integrated view. *Langmuir* **2006**, *22* (8), 3497−3505.

(19) Huang, J.; Buboltz, J. T.; Feigenson, G. W. Maximum solubility of cholesterol in phosphatidylcholine and phosphatidylethanolamine bilayers. *Biochimica et Biophysica Acta (BBA)-Biomembranes* **1999**, *1417* (1), 89−100.

(20) Buboltz, J. T.; Feigenson, G. W. A novel strategy for the preparation of liposomes: rapid solvent exchange. *Biochimica et Biophysica Acta (BBA)-Biomembranes* **1999**, *1417* (2), 232−245.

(21) Ibarguren, M.; Alonso, A.; Tenchov, B. G.; Goñi, F. M. Quantitation of cholesterol incorporation into extruded lipid bilayers. *Biochimica et Biophysica Acta (BBA)-Biomembranes* **2010**, *1798* (9), 1735−1738.

(22) Sundh, M.; Svedhem, S.; Sutherland, D. S. Influence of phase separating lipids on supported lipid bilayer formation at SiO2 surfaces. *Phys. Chem. Chem. Phys.* **2010**, *12* (2), 453−460.

(23) Evans, E.; Rawicz, W. Entropy-driven tension and bending elasticity in condensed-fluid membranes. *Phys. Rev. Lett.* **1990**, *64* (17), 2094.

(24) Redondo-Morata, L.; Giannotti, M. I.; Sanz, F. Influence of Cholesterol on the Phase Transition of Lipid Bilayers: A Temperature-Controlled Force Spectroscopy Study. *Langmuir* **2012**, *28* (35), 12851−12860.

(25) Shamitko-Klingensmith, N.; Molchanoff, K. M.; Burke, K. A.; Magnone, G. J.; Legleiter, J. Mapping the mechanical properties of cholesterol-containing supported lipid bilayers with nanoscale spatial resolution. *Langmuir* **2012**, *28* (37), 13411−13422.

(26) Cho, N. J.; Cho, S. J.; Cheong, K. H.; Glenn, J. S.; Frank, C. W. Employing an amphipathic viral peptide to create a lipid bilayer on Au and TiO_2. *J. Am. Chem. Soc.* **2007**, *129* (33), 10050−1.

(27) Hardy, G. J.; Nayak, R.; Munir Alam, S.; Shapter, J. G.; Heinrich, F.; Zauscher, S. Biomimetic supported lipid bilayers with high cholesterol content formed by α-helical peptide-induced vesicle fusion. *J. Mater. Chem.* **2012**, *22* (37), 19506−19513.

(28) Simonsson, L.; Gunnarsson, A.; Wallin, P.; Jönsson, P.; Höök, F. Continuous lipid bilayers derived from cell membranes for spatial molecular manipulation. *J. Am. Chem. Soc.* **2011**, *133* (35), 14027−14032.

(29) Simonsson, L.; Höök, F. Formation and Diffusivity Characterization of Supported Lipid Bilayers with Complex Lipid Compositions. *Langmuir* **2012**, *28* (28), 10528−10533.

(30) Hohner, A. O.; David, M. P. C.; Rädler, J. O. Controlled solvent-exchange deposition of phospholipid membranes onto solid surfaces. *Biointerphases* **2010**, *5* (1), 1−8.

(31) Szoka, F.; Papahadjopoulos, D. Procedure for preparation of liposomes with large internal aqueous space and high capture by reverse-phase evaporation. *Proc. Natl. Acad. Sci. U. S. A.* **1978**, *75* (9), 4194−4198.
(32) Cornell, B.; Braach-Maksvytis, V.; King, L.; Osman, P.; Raguse, B.; Wieczorek, L.; Pace, R. A biosensor that uses ion-channel switches. *Nature* **1997**, 580−582.
(33) Heinrich, F.; Ng, T.; Vanderah, D. J.; Shekhar, P.; Mihailescu, M.; Nanda, H.; Lösche, M. A New Lipid Anchor for Sparsely Tethered Bilayer Lipid Membranes†. *Langmuir* **2009**, *25* (7), 4219−4229.
(34) Tabaei, S. R.; Choi, J. H.; Haw Zan, G.; Zhdanov, V. P.; Cho, N.-J. Solvent-Assisted Lipid Bilayer Formation on Silicon Dioxide and Gold. *Langmuir* **2014**.
(35) MacDonald, R. C.; MacDonald, R. I.; Menco, B. P. M.; Takeshita, K.; Subbarao, N. K.; Hu, L.-r. Small-volume extrusion apparatus for preparation of large, unilamellar vesicles. *Biochimica et Biophysica Acta (BBA)-Biomembranes* **1991**, *1061* (2), 297−303.
(36) Jönsson, P.; Jonsson, M. P.; Tegenfeldt, J. O.; Höök, F. A method improving the accuracy of fluorescence recovery after photobleaching analysis. *Biophys. J.* **2008**, *95* (11), 5334−5348.
(37) Keller, C.; Kasemo, B. Surface specific kinetics of lipid vesicle adsorption measured with a quartz crystal microbalance. *Biophys. J.* **1998**, *75* (3), 1397−1402.
(38) Beseničar, M. P.; Bavdek, A.; Kladnik, A.; Maček, P.; Anderluh, G. Kinetics of cholesterol extraction from lipid membranes by methyl-*β*-cyclodextrin—a surface plasmon resonance approach. *Biochimica et Biophysica Acta (BBA)-Biomembranes* **2008**, *1778* (1), 175−184.
(39) Cremer, P. S.; Boxer, S. G. Formation and spreading of lipid bilayers on planar glass supports. *J. Phys. Chem. B* **1999**, *103* (13), 2554−2559.
(40) Sauerbrey, G. Verwendung von Schwingquarzen zur Wägung dünner Schichten und zur Mikrowägung. *Zeitschrift für Physik* **1959**, *155* (2), 206−222.
(41) Radhakrishnan, A.; McConnell, H. M. Chemical activity of cholesterol in membranes. *Biochemistry* **2000**, *39* (28), 8119−8124.
(42) McConnell, H. M.; Radhakrishnan, A. Condensed complexes of cholesterol and phospholipids. *Biochimica et Biophysica Acta (BBA)-Biomembranes* **2003**, *1610* (2), 159−173.
(43) Raguz, M.; Mainali, L.; Widomska, J.; Subczynski, W. K. The immiscible cholesterol bilayer domain exists as an integral part of phospholipid bilayer membranes. *Biochimica et Biophysica Acta (BBA)-Biomembranes* **2011**, *1808* (4), 1072−1080.
(44) Mainali, L.; Raguz, M.; Subczynski, W. K. Formation of Cholesterol Bilayer Domains Precedes Formation of Cholesterol Crystals in Cholesterol/Dimyristoylphosphatidylcholine Membranes: EPR and DSC Studies. *J. Phys. Chem. B* **2013**, *117* (30), 8994−9003.
(45) Tulenko, T. N.; Chen, M.; Mason, P. E.; Mason, R. P. Physical effects of cholesterol on arterial smooth muscle membranes: evidence of immiscible cholesterol domains and alterations in bilayer width during atherogenesis. *J. Lipid Res.* **1998**, *39* (5), 947−956.
(46) Jacob, R. F.; Cenedella, R. J.; Mason, R. P. Direct evidence for immiscible cholesterol domains in human ocular lens fiber cell plasma membranes. *J. Biol. Chem.* **1999**, *274* (44), 31613−31618.
(47) Anderton, C. R.; Lou, K.; Weber, P. K.; Hutcheon, I. D.; Kraft, M. L. Correlated AFM and NanoSIMS imaging to probe cholesterol-induced changes in phase behavior and non-ideal mixing in ternary lipid membranes. *Biochimica et Biophysica Acta (BBA)-Biomembranes* **2011**, *1808* (1), 307−315.
(48) Wilson, R. L.; Kraft, M. L. Quantifying the Molar Percentages of Cholesterol in Supported Lipid Membranes by Time-of-Flight Secondary Ion Mass Spectrometry and Multivariate Analysis. *Anal. Chem.* **2012**, *85* (1), 91−97.